

(c) $\alpha_1 = 15^\circ$

(d) $\alpha_1 = 20^\circ$

Fig. 8 The Speed Profile in Yaw

It can be seen from the first four curves that the speed difference of two sides of blade rises obviously as the yaw angle increasing, the maximum of which is about $1.6m/s$. The area behind the front two wind turbines is more affected by the first one in the first row. Therefore, the region of the rear wind turbine in the wakes of the first one in the first row is larger increasingly as increase of the yaw angle. The flow field become more complex in the area closed to the first one combined with effect of the rear one, while the other region is stable relatively. Besides, the wind speed in the far field in the different yaw angles are similar.

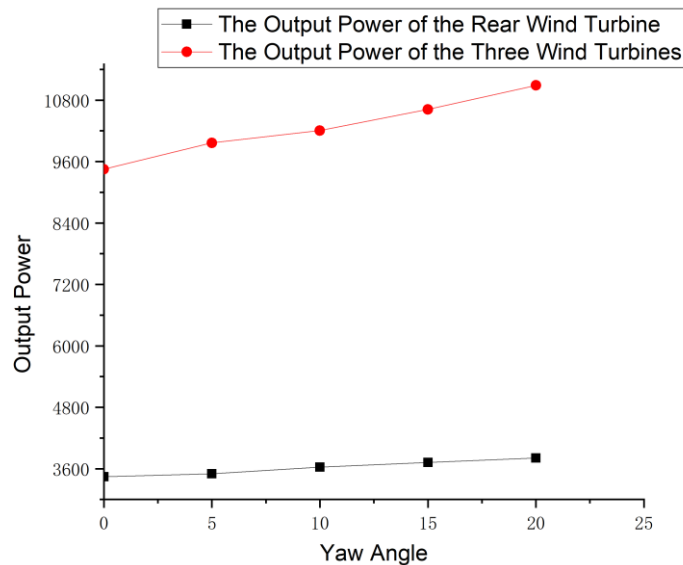


Fig. 9 Total Output Power

As the yaw angle increasing, the output power of the downstream wind turbine increases continuously. Especially when the yaw angle reaches to 20° , the output power is up to the maximum. In the period of the yaw angle increases, the downstream one gradually changes from the state that the two upstream wind turbines commonly affect it to the state that the first one influences its incoming flow mainly by the wake of

the first one. On the one hand, yaw angle can change the flow direction of wind turbines and affect the whole flow field distribution. On the other hand, it increases the distance where the wake of the upstream one affects the downstream one, and reduces the turbulence intensity caused by wake interference. Therefore, the output power of the downstream one is improved relatively.

Theoretically, when yaw angle exceeds a limit value, it is almost completely in the wake area of the first upstream one. And its output power may reduce relatively, but the results is not presented like that. One of the possible reasons is that the yaw angle studied may be not wide enough. And the second one is that the influence of the distance between the first front one and the rear one may be much more than that of whether it is totally behind the wakes area of the first front one. When there is no yaw and the stagger distance is zero, the downstream one is located directly behind the wake area of the first one as well. However, when yaw angle reaches to 20° , the output power is even lower due to its higher turbulence intensity, compared with the former.

5. CONCLUSIONS

In the case of maintaining the fixed space between the different rows and ranks in the wind farm, the flow characteristics and facilities performance of the three wind turbines with inverted-triangle distribution are researched by adopting ALM. The optimum stagger distance without yaw is obtained by changing the relative distance between the downstream wind turbine and the first wind turbine in the upstream. Based on it, the influence of wakes superposition of the two upstream wind turbines in the case of yaw is considered.

The numerical simulation illustrated that the wakes interference effect of the two upstream wind turbines is extremely remarkable. In the case of no yaw, the rear wind turbine is gradually situated from the wakes zone of the first one in the front row to the wake interference zone of the two wind turbines as the stagger distance between the first wind turbine in the first row and downstream one increasing. The growth rate of the output power is improved relatively to the previous process. However, the improvement is limited due to the wake interference effect. Especially when the stagger distance reaches at $4D/3$, the power growth and total power are up to the maximum.

As the yaw angle increasing, the output power of the downstream wind turbine increases continuously, and the output power is up to the maximum, when the yaw angle reaches to 20° . In the period of the yaw angle increases, the downstream one gradually changes from the state that the two upstream wind turbines commonly affect it to the state that the first one influences its incoming flow mainly by the wake of the first one.

According to the wind speed profile above, the interference scope of two wind turbines in the same row could be determined in the case of no yaw. Meanwhile, the optimum stagger distance without yaw can be obtain. Also, the situations of different angles could be analyzed. It could provide a reference value to spatial layout of the complete wind farm.

REFERENCES

1. Leung, D.Y.C. and Y. Yang (2012). *Wind energy development and its environmental impact: A review*. Renewable & Sustainable Energy Reviews. **16**(1): p. 1031-1039.
2. Vermeer, L.J., J.N. Sørensen, and A. Crespo (2003). *Wind turbine wake aerodynamics*. Progress in Aerospace Sciences. **39**(6): p. 467-510.
3. Sande, B., S.P. Pijl, and B. Koren (2011). *Review of computational fluid dynamics for wind turbine wake aerodynamics*. Wind Energy. **14**(7): p. 799-819.
4. Lee, S., et al. (2011). *Atmospheric and Wake Turbulence Impacts on Wind Turbine Fatigue Loadings*. Boundary Layers. **135**(3): p. 14-16.
5. Kim, S.H., et al. (2015). *A study of the wake effects on the wind characteristics and fatigue loads for the turbines in a wind farm*. Renewable Energy. **74**: p. 536-543.
6. Shenkar, R. (2010). *Design and Optimization of Planar and Nonplanar Wind Turbine Blades Using Vortex Methods Master Thesis*.
7. Jimenez, A., et al. (2007). *Advances in large-eddy simulation of a wind turbine wake*.
8. Jiménez, Á., A. Crespo, and E. Migoya (2010). *Application of a LES technique to characterize the wake deflection of a wind turbine in yaw*. Wind Energy. **13**(6): p. 559-572.
9. KROGSTAD, et al. (2013). *Blind test calculations of the performance and wake development for a model wind turbine*. Renewable Energy. **50**: p. 325-333.
10. PIERELLA, et al. (2014). *Blind Test 2 calculations for two in-line model wind turbines where the downstream turbine operates at various rotational speeds*. Renewable Energy. **70**(5): p. 62-77.
11. Krogstad, P.Å., L. Sætran, and M.S. Adaramola (2015). *"Blind Test 3" calculations of the performance and wake development behind two in-line and offset model wind turbines*. Journal of Fluids & Structures. **52**(1): p. 65-80.
12. Fleming, P., et al. (2015). *Simulation comparison of wake mitigation control strategies for a two-turbine case*. Wind Energy, 2015. **18**(12): p. 2135-2143.
13. Draper, M., et al. (2018). *A Large Eddy Simulation-Actuator Line Model framework to simulate a scaled wind energy facility and its application*. Journal of Wind Engineering and Industrial Aerodynamics. **182**: p. 146-159.
14. Sørensen, J.N.R. and W.Z. Shen (2002). *Numerical Modeling of Wind Turbine Wakes*. Journal of Fluids Engineering. **124**(2): p. 393.
15. JangOh, CHOUDHRY, Amanullah, et al. (2013). *Large eddy simulation of the wind turbine wake characteristics in the numerical wind tunnel model[J]*. Journal of Wind Engineering & Industrial Aerodynamics. **112**(112):11-24.
16. Wang Shengjun. (2014). *Research on Wake Characteristics of Wind Turbine Based on Actuator Line Model [D]*. Graduate School of Chinese Academy of Sciences (Institute of Engineering Thermophysics).
17. Ai Yong, Cheng Ping, Wan Decheng. (2018). *Numerical Simulation of Wake Field of Two Stagger Wind Turbines Based on Actuator Line Model [J]*. Ocean engineering. **36**(01):27-36